

RmGPT: Rotating Machinery Generative Pretrained Model

Yilin Wang^a, Yifei Yu^a, Kong Sun^a, Peixuan Lei^a, Yuxuan Zhang^a, Enrico Zio^{b,c}, Aiguo Xia^d, Yuanxiang Li^{a,*}

^a*School of Aeronautics and Astronautics, Shanghai Jiao Tong University, Shanghai, China*

^b*MINES Paris-PSL University, Paris, France*

^c*Energy Department, Politecnico di Milano, Milano, Italy*

^d*Beijing Aeronautical Technology Research Center, Beijing, China*

Abstract

In industry, the reliability of rotating machinery is critical for production efficiency and safety. Current methods of Prognostics and Health Management (PHM) often rely on task-specific models, which face significant challenges in handling diverse datasets with varying signal characteristics, fault modes and operating conditions. Inspired by advancements in generative pretrained models, we propose RmGPT, a unified model for diagnosis and prognosis tasks. RmGPT introduces a novel token-based framework, incorporating Signal Tokens, Prompt Tokens, Time-Frequency Task Tokens and Fault Tokens to handle heterogeneous data within a unified model architecture. We leverage self-supervised learning for robust feature extraction and introduce a next signal token prediction pretraining strategy, alongside efficient prompt learning for task-specific adaptation. Extensive experiments demonstrate that RmGPT significantly outperforms state-of-the-art algorithms, achieving near-perfect accuracy in diagnosis tasks and exceptionally low errors in prognosis tasks. Notably, RmGPT excels in few-shot learning scenarios, achieving 92% accuracy in 16-class one-shot experiments, highlighting its adaptability and robustness. This work establishes RmGPT as a powerful PHM foundation model for rotating machinery, advancing the scalability and generalizability of PHM solutions.

Keywords: Rotating Machinery, Reliability, Prognostics and Health Management, Remaining Useful Life Prediction, Fault Diagnosis, Foundation Model, Self-supervised Learning

1. Introduction

Rotating machinery is a critical component in many industrial applications[1, 2], and ensuring its reliability is essential for production efficiency and safety[3]. Prognostics and Health Management (PHM) encompasses a range of methodologies aimed at assessing and predicting the present and future health status of equipment[4, 5]. The outcomes of PHM enable timely maintenance to prevent unexpected failures. Current PHM methods for fault diagnosis and prognosis often rely on task-specific models tailored to particular types of equipment and operational conditions and specific fault modes.

*Corresponding author: School of Aeronautics and Astronautics, Shanghai Jiao Tong University, Shanghai 200240, China. Tel: +86 21-34206160.

Email addresses: pandalin@sjtu.edu.cn (Yilin Wang), yuyifei@sjtu.edu.cn (Yifei Yu), mr_sun@sjtu.edu.cn (Kong Sun), lei.2333@sjtu.edu.cn (Peixuan Lei), yuxuanzhang@sjtu.edu.cn (Yuxuan Zhang), enrico.zio@polimi.it (Enrico Zio), xag14@tsinghua.org.cn (Aiguo Xia)

They typically involve handcrafted features and machine learning algorithms designed to identify specific fault patterns from historical data[6, 7, 8].

While effective in specific contexts, these task-specific models encounter significant challenges when applied to diverse datasets with varying signal characteristics, fault modes, and operating environments[9]. Several key difficulties arise in this context: **1) Variability in Signal Dynamics:** Different types of diagnosis equipment exhibit significant variations in sensor quantity, installation position, monitored types of signals, and sampling frequencies. Modeling these diverse signals within a unified framework is highly challenging. **2) Diversity in Fault Mechanisms and Patterns:** The wide range of equipment types and their differing designs and fault mechanisms complicate the definition of unified diagnosis and prognosis tasks. Each equipment type may exhibit unique fault behaviors that are difficult to generalize across other types. **3) Lack of a Foundation Model for Rotating Machinery:** The differences in input signals and diagnostic tasks lead to the difficulty of having a foundation model capable of using a single set of parameters to effectively perform diagnosis and prognosis tasks across multiple types of equipment. Despite efforts by researchers to employ transfer learning techniques for domain adaptation and generalization in rotating machinery[10, 11, 12, 13, 14], the absence of such a foundation model limits knowledge transfer and sharing between different devices and hinders the application of AI techniques in real PHM scenarios[15].

Inspired by advancements in generative pretrained models like ChatGPT [16] and SAM [17], we propose RmGPT, a unified model for diagnosis and prognosis tasks in rotating machinery. RmGPT leverages self-supervised learning to capture generalizable features from vast amounts of unlabeled data and introduces a unified diagnosis and prognosis framework that integrates data and tasks from different diagnosis equipment into a generative token-based paradigm. By using a consistent model architecture and parameters, RmGPT can effectively handle the heterogeneity of rotating machinery data, encompassing various signal channels, fault categories, sampling frequencies and dataset sizes. This novel approach, illustrated in Fig. 1, not only simplifies the model development process but also enhances the model robustness and adaptability in real-world applications, demonstrating superior generalization across different types of equipment and operational conditions.

In this paper, we present several key contributions:

- 1. Unified Diagnosis and Prognosis Paradigm:** We propose a novel paradigm based on a semantic token space for diagnosis and prognosis. This involves using learnable Fault Tokens to capture fault prototypes of different equipment and Time-Frequency Task Tokens to represent the health status semantics of input signals. Unified diagnosis and prognosis are performed by comparing these health status semantics tokens with Fault Tokens.
- 2. Unified Efficient Model for Diagnosis and Prognosis:** We introduce an efficient model that can adaptively handle different signal inputs. The model utilizes learnable Prompt Tokens to adaptively learn sensor semantic features from different equipment and employs an efficient Signal Token mapping method, with a dual-stage attention mechanism to efficiently and adaptively extract signal semantics. Additionally, we propose a Next Signal Token Prediction pretraining strategy to

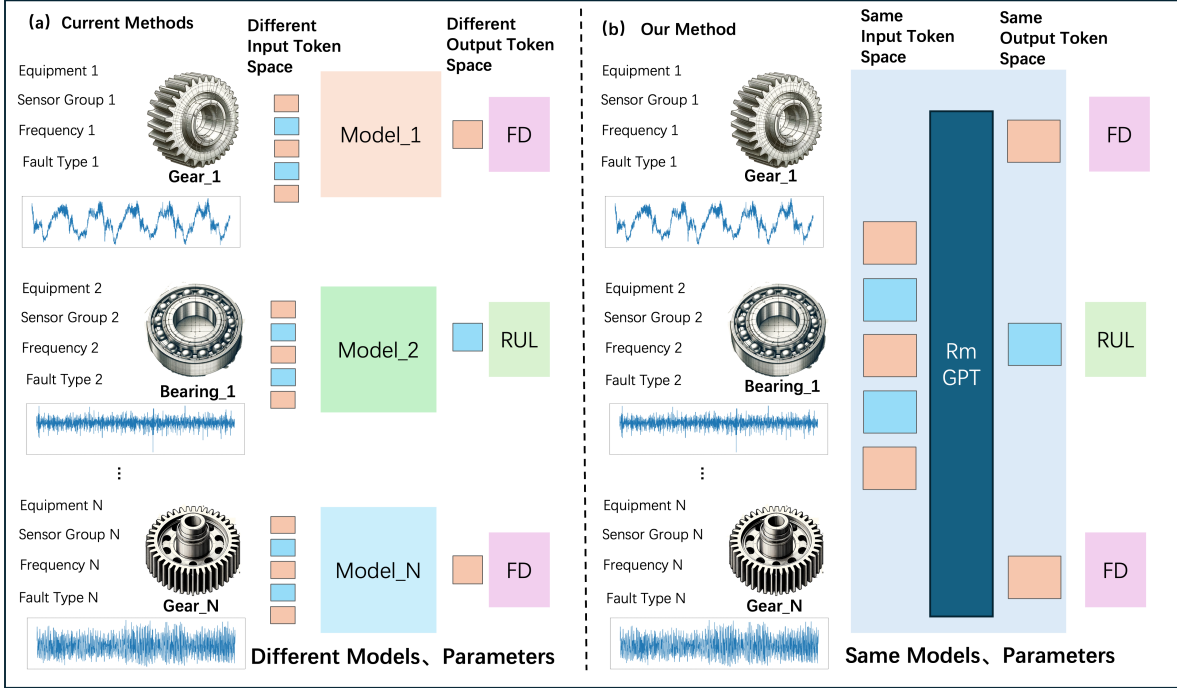


Figure 1: Unlike current research methods that use different models for different equipment, this study uses the same model parameters to address cross-condition diagnosis and prognosis for rotating machinery with varying sensors, frequencies, and fault modes.

capture generalizable features from vast amounts of unlabeled data and an Efficient Prompt Learning method for high-efficiency task adaptation.

3. Superior Performance Across Diverse Datasets: Extensive experiments demonstrate that RmGPT significantly outperforms state-of-the-art (SOTA) algorithms in both diagnosis and prognosis tasks. The model achieves near-perfect accuracy in diagnosis tasks and exceptionally low errors in prognosis tasks. Additionally, RmGPT shows remarkable performance in few-shot learning scenarios, achieving high accuracy even with minimal training samples, thus validating its adaptability and robustness.

The remainder of this paper is structured as follows. Section II describes the problem definition and the proposed RmGPT model. Section III details the training process, including pretraining and prompt learning. Section IV presents the experimental setup and results, highlighting the model’s performance across various tasks. Finally, Section V concludes the paper with a summary of our findings and directions for future research.

2. Problem Definition

We consider PHM tasks of diagnosis and prognosis for rotating machinery. Different equipment generate datasets $D = \{D_i \mid i = 1, \dots, n\}$, each described as $D_i = (\mathcal{X}_i, \mathcal{Y}_i)$, where \mathcal{X}_i and \mathcal{Y}_i represent the time series of the input signals and the corresponding task outputs, respectively. Each \mathcal{X}_i consists of sensor monitored signals with varying dimensions M_i , different frequencies f_i , distinct operational

conditions, and various task types \mathcal{Y}_i . The datasets D_i , thus, exhibit significant heterogeneity. Traditional methods have individually defined the inputs and outputs of the problem for specific operational conditions and fault types of a particular device or class of equipment. This Section attempts to offer a description of the diagnosis and prognosis tasks of different D_i in a unified form.

2.1. Self-Supervised Learning for Foundation Models

Different from a model $\mathcal{Y}_i = F_i(\mathcal{X}_i; \theta_i)$ and its parameters θ_i for specific data D_i , we aim to find a foundation model $Y = F(\mathcal{X}; \theta)$ for all rotating machinery datasets D . A feasible approach is to leverage the powerful capabilities of self-supervised learning, which excels in learning robust representations from unlabeled data and unifying diverse tasks and conditions.

In self-supervised learning, a pretext task T_p is designed to train the model using unlabeled data \mathcal{X} . The objective is to learn a general representation $\mathbf{h} = F(\mathcal{X}; \theta_e)$, where θ_e are the pretraining parameters. The representation \mathbf{h} is then used to solve the pretext task T_p , typically by predicting some part of the input \mathcal{X} based on the rest. Formally, the self-supervised learning objective is:

$$\theta_e = \arg \min_{\theta_e} \mathbb{E}_{\mathcal{X} \sim D} [\mathcal{L}_{T_p}(\mathcal{X}, F(\mathcal{X}; \theta_e))], \quad (1)$$

where \mathcal{L}_{T_p} is the loss function associated with the pretext task T_p . Once pre-trained, the model F and representation \mathbf{h} can be fine-tuned on downstream diagnosis and prognosis tasks using labeled data \mathcal{Y} . This pretraining on extensive unlabeled data enables the model to learn generalized features, making it adaptable for various diagnosis and prognosis tasks, thus providing a comprehensive and flexible framework for rotating machinery PHM.

2.1.1. Diagnosis and Prognosis

Building on the general representation \mathbf{h} obtained through pretraining, we define the mapping relationship for task outputs as:

$$\hat{\mathcal{Y}}_i = \arg \max_{\mathcal{Y}_i} P(\mathcal{Y}_i | \mathbf{h}_i, \theta_d), \quad (2)$$

where $\hat{\mathcal{Y}}_i$ is the predicted output for dataset D_i based on the learned tokens \mathbf{h}_i and the same foundation model F with the same parameters θ_d . For the diagnosis task, $Y_i \in \mathbb{R}^{FC_i}$, the model outputs a classification among the fault categories FC_i . For the prognosis task, $Y_i \in \mathbb{R}$, the model outputs a Remaining Useful Life (RUL) prediction.

2.1.2. Prompt Learning & Finetuning

Prompt learning and finetuning are two approaches to adapt the foundation model to downstream tasks, with different optimization parameters.

For prompt learning, task-specific prompts \mathbf{p} are introduced to guide the model's adaptation:

$$\theta_p = \arg \min_{\theta_p} \mathbb{E}_{(\mathcal{X}_i, \mathcal{Y}_i) \sim D} [\mathcal{L}(\mathcal{Y}_i, F(\mathcal{X}_i, \mathbf{p}; \theta_e))], \quad (3)$$

where θ_e are the pretrained parameters and θ_p are the parameters for prompt adaptation. The prompts \mathbf{p} help the model leverage the pretrained representations effectively for specific tasks.

For finetuning, the model parameters θ_f are directly adjusted based on the labeled data:

$$\theta_f = \arg \min_{\theta_f} \mathbb{E}_{(\mathcal{X}_i, \mathcal{Y}_i) \sim D} [\mathcal{L}(\mathcal{Y}_i, F(\mathcal{X}_i; \theta_f))], \quad (4)$$

notably the finetuned parameters θ_f and θ_p are the same for all the data and tasks.

2.1.3. Few-shot Learning & One-Shot Learning

Few-shot learning enables the model to perform well with limited labeled data. The objective is defined as:

$$\theta_{fs} = \arg \min_{\theta_{fs}} \mathbb{E}_{(\mathcal{X}_i, \mathcal{Y}_i) \sim D_{fs}} [\mathcal{L}(\mathcal{Y}_i, F(\mathcal{X}_i; \theta_e, \theta_{fs}))], \quad (5)$$

where θ_{fs} are the parameters optimized using few-shot examples from D_{fs} , a subset of D with few labeled samples. In particular, when each fault category in D_{fs} has only one sample, the task becomes one-shot learning.

3. Rotating Machinery Generative Pretrained Model

In this chapter, we introduce RmGPT, as depicted in Fig. 2. RmGPT serves as a foundation model for unified diagnosis and prognosis of rotating machinery. The model employs a generative framework using tokens to represent diagnosis and prognosis tasks. It features an optimized architecture with a patch-based tokenizer and a time-channel attention transformer, ensuring efficient processing and adaptability. The training process includes a pretrained strategy focused on predicting signal tokens and a prompt-based technique for fine-tuning the model to specific tasks.

3.1. Unified Diagnosis and Prognosis Framework

To develop a foundation model that unifies the modeling of \mathcal{X} and the diagnosis and prognosis \mathcal{Y} , we draw inspiration from large language models and multimodal frameworks, proposing the use of tokens to represent diverse data and task information. Unlike conventional approaches that require separate models for different datasets or tasks, RmGPT employs a unified architecture and set of parameters to model signals \mathcal{X}_i from various equipment, sensor groups, frequencies, and operational conditions, along with their corresponding diagnosis and prognosis outputs \mathcal{Y}_i for different fault categories, all within a cohesive token space.

We integrate the diagnosis and prognosis tasks of different equipment into a unified token sequence, where each token in the sequence is designed to represent specific types of information, as depicted in Fig.3a. At the beginning of the sequence, Prompt Tokens are introduced to enhance the model's adaptability by embedding task-specific statistical information, enabling seamless integration of context-aware knowledge. The middle of the sequence is composed of Signal Tokens, which capture the essential trends and patterns within the input signals, ensuring consistency and stability across varying scales and sensor configurations. Towards the end of the sequence, Time-Frequency Task Tokens are designed to encapsulate the health semantics of the input data, providing a strong foundation for both diagnosis and prognosis tasks. Finally, Fault Tokens represent the prototype characteristics of different fault

modes, facilitating precise fault detection and Remaining RUL prediction through a comparison-based approach. This structured token sequence allows for the execution of various downstream tasks based on the relationships between these tokens.

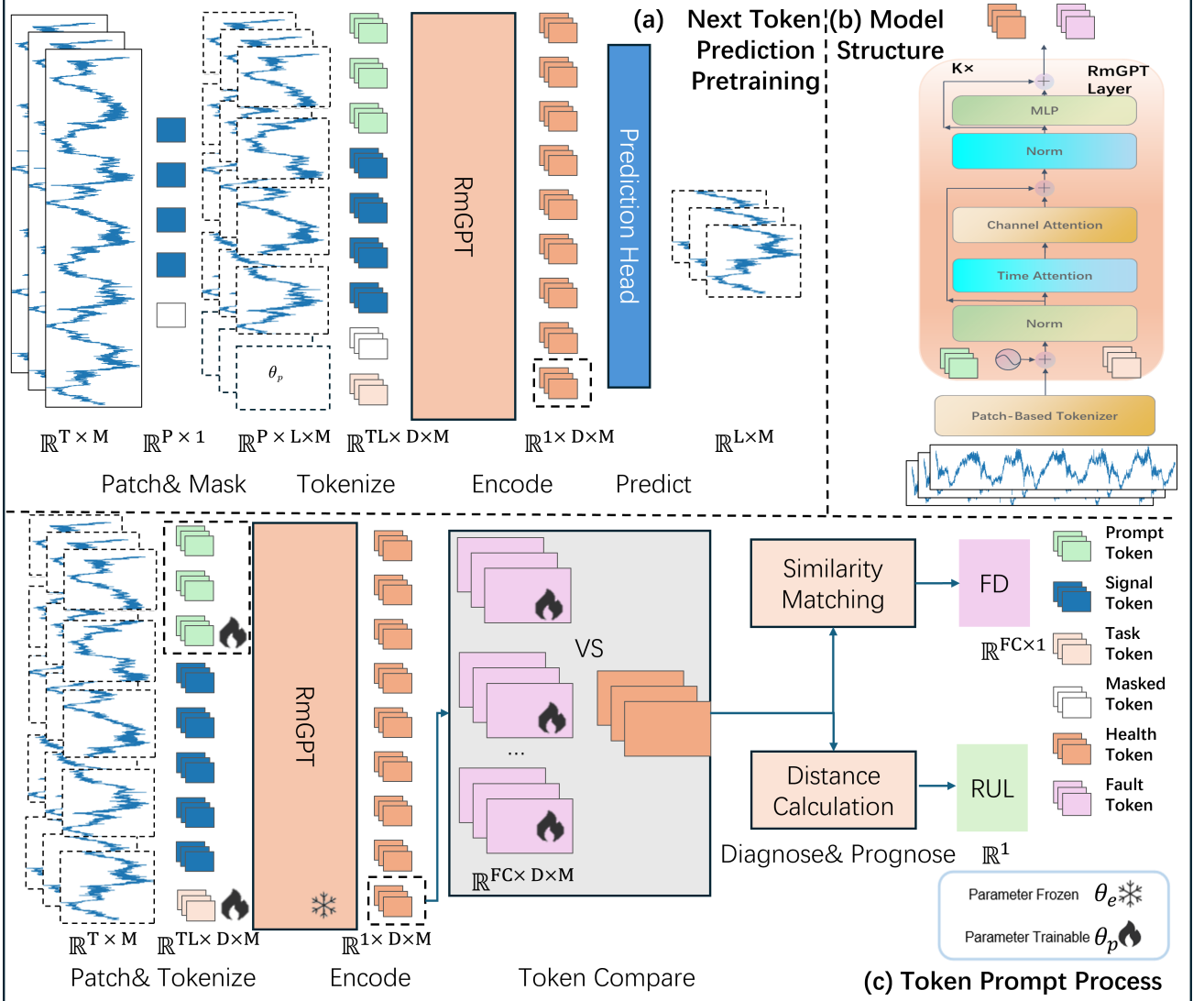


Figure 2: The proposed foundation model for diagnosis and prognosis, RmGPT, includes: (a) a pretraining strategy for predicting future signal tokens, (b) the internal architecture of RmGPT, and (c) a generalized paradigm for diagnosis and prognosis based on generative tokens and the prompt technique.

3.1.1. Prompt Tokens

Prompt tokens $T_p \in \mathbb{R}^{l_p \times M_i \times d}$ are crafted as a combination of sequence time-domain statistical information and learnable embeddings, where l_p denotes the length of the prompt token sequence, M_i represents the number of signal channels for different equipment, and d corresponds to the number of hidden units in the model. This dual-purpose design allows the model to effectively capture and utilize key statistical features of the input signals. Specifically, the extracted signal mean and variance are

integrated into the token space, thereby enhancing the model’s ability to perceive and process statistical nuances while maintaining a focus on the morphological characteristics of the signals. Furthermore, in scenarios involving multiple equipment and tasks, each dataset and task is assigned its own set of learnable prompt tokens. These tokens are tailored to incorporate context-specific knowledge, thus helping the model distinguish between different equipment conditions and tasks. This design ensures that the model remains adaptable and context-aware, providing a robust foundation for accurate diagnosis and prognosis across a wide range of scenarios.

3.1.2. Signal Tokens

To ensure that the signal tokens $T_s \in \mathbb{R}^{l_s \times M_i \times d}$ effectively capture the trends within the signals and maintain stability across varying scales, we first standardize the input signals by normalizing their mean and variance, where l_s represents the length of the signal token sequence. This standardization step helps to stabilize the numerical values of the signals, ensuring consistency and reliability in the token representation. Furthermore, to provide more robust and coherent semantics for each token block, we segment the long time series signals into several sub-sequences, mapping each sub-sequence into a fixed-dimensional token space. Given that different equipment may have varying numbers of sensor channels M_i , we preserve the channel dimension’s shape, allowing the model to process data from different channel configurations within a unified framework. Additionally, we propose a flexible network structure that can dynamically adapt to these varying channel numbers, further enhancing the model’s ability to generalize across diverse datasets and equipment types.

3.1.3. Time-Frequency Task Tokens & Health Token

Time-Frequency task tokens $T_t \in \mathbb{R}^{l_t \times M_i \times d}$ are designed for general representation learning across various tasks and can adapt to any diagnosis and prognosis tasks, where l_t represents the length of the task token sequence. These tokens combine learnable embeddings and frequency-domain representations of the input signals. The input signals are transformed using the Fast Fourier Transform (FFT) to obtain the signal’s spectrum and phase, which are then projected into the token space to get frequency-domain representations. A learnable embedding is concatenated before the frequency-domain representation to form the Time-Frequency task tokens. These tokens, containing task characteristics, are fed into the foundation model to produce Health Tokens $T_h \in \mathbb{R}^{l_t \times M_i \times d}$, representing the health state of the input signals for downstream tasks (Fig. 2c).

3.1.4. Fault Tokens

Fault tokens $T_f \in \mathbb{R}^{FC_i \times l_t \times M_i \times d}$ are introduced to address the challenges of generalizing fault diagnosis and prognosis across different equipment types and operational conditions. Here, FC_i represents the fault types of the i^{th} equipment, where a vector of shape $\mathbb{R}^{l_t \times M_i \times d}$ is stored for each fault type, encapsulating the characteristics of each channel under the respective fault condition. These tokens are designed as learnable embeddings that autonomously capture the prototype characteristics of various sensor channels under specific fault conditions during extensive data learning. The motivation

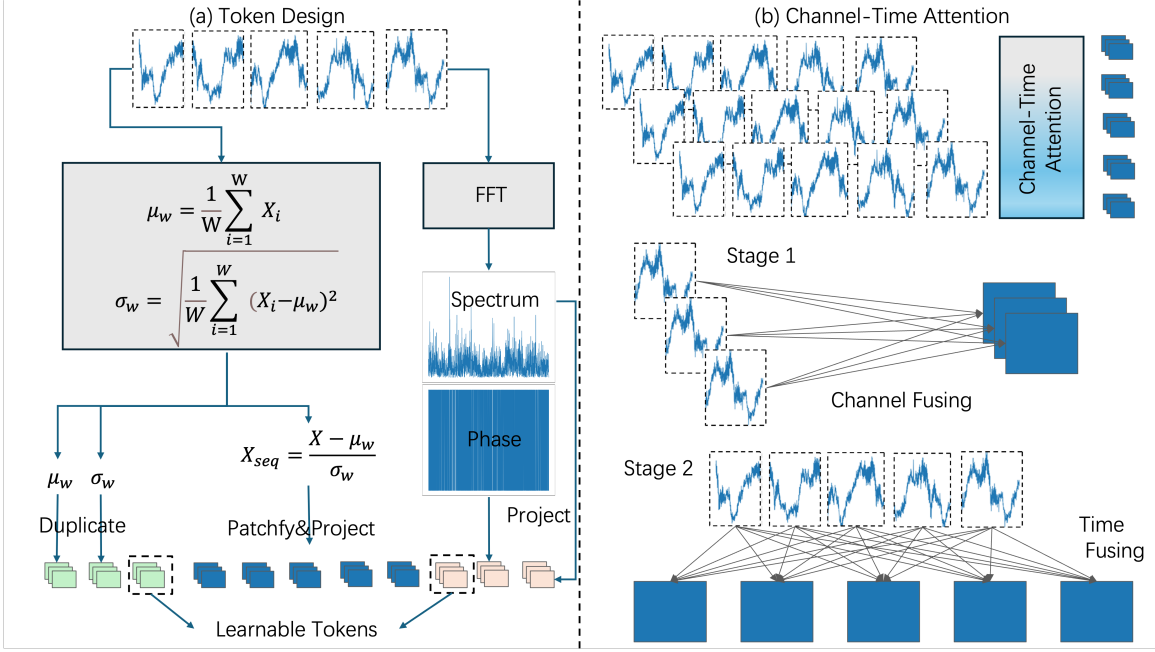


Figure 3: (a) Unified token design in the model’s token space. (b) Channel-Time Attention mechanism for efficient aggregation of variable-length and multi-channel signals.

behind using fault tokens lies in their ability to encapsulate the essential features of different fault modes, making them highly effective for tasks involving classification and prediction of RUL. By representing fault modes as prototype embeddings, the model can more accurately distinguish between different types of faults, even when the input signals vary significantly across equipment. This approach ensures that the diagnosis and prognosis tasks are grounded in the most relevant features of the fault, thereby enhancing the overall interpretability and robustness of the model.

To implement the diagnosis and prognosis tasks, a comparison-based approach is utilized, wherein the health representations T_h are compared against the fault tokens T_f . For diagnosis tasks, the model calculates the similarity between T_h and each fault prototype representation in FC_i , selecting the fault category with the highest similarity as the diagnosis result. In the context of RUL prediction, the Euclidean distance between T_h and each fault prototype representation in FC_i is computed, with the minimum distance being transformed into the predicted RUL. This comparison-based method is driven by its flexibility and adaptability to various input scenarios, enabling the model to seamlessly handle diverse diagnostic and prognostic tasks. Furthermore, this approach provides more interpretable results, as the diagnosis and prognosis are directly linked to the specific characteristics of the identified fault mode.

3.2. Model Architecture

The RmGPT model is meticulously designed to achieve efficient processing of input/output data while maintaining a high degree of flexibility and generality. The architecture incorporates several innovative components that contribute to its robust performance across various diagnostic and prognostic

tasks, regardless of the equipment involved.

3.2.1. Patch-Based Tokenizer

The Patch-Based Tokenizer plays a crucial role in segmenting input signals into manageable patches[18], transforming local information into semantic vectors suitable for processing by the Transformer network, as depicted in Fig. 3a. For a multivariate time series $x^i \in \mathbb{R}^{L_i \times M_i}$, this process involves dividing the signal into patches of length P with a stride S , resulting in N_i patches:

$$N_i = \left\lfloor \frac{L_i - P}{S} \right\rfloor + 1 \quad (6)$$

Each patch $x_p^{(i)}$ is then linearly transformed into a token $x_t^{(i)} \in \mathbb{R}^{N_i \times d \times M_i}$:

$$x_t^{(i)} = \text{Linear}(x_p^{(i)}) \quad (7)$$

Position encoding W_{pos} is added to these tokens to incorporate temporal information, resulting in the signal tokens $T_s^{(i)}$:

$$T_s^{(i)} = x_t^{(i)} + W_{pos} \quad (8)$$

This tokenization approach significantly reduces the computational and memory requirements, which typically scale with the square of the sequence length N in a Transformer network [19]. By reducing N from the full length of the input sequence L to approximately $\frac{L}{S}$, this method achieves a quadratic reduction in complexity. For example, in our dataset, an input sequence of length $L = 2048$ is divided into patches of length $P = 256$ with a stride of $S = 256$, thereby significantly lowering the computational burden while preserving the semantic integrity of each token.

3.2.2. Channel-Time Attention Transformer

A key innovation in the RmGPT architecture is the Channel-Time Attention Transformer, which is designed to handle the variability in input data effectively while reducing computational complexity. This mechanism is motivated by the need to process multi-channel rotating machinery data efficiently.

The Channel-Time Attention Transformer operates through a two-stage attention mechanism, which is crucial for enabling the model to efficiently process signals from any combination of sensor channels. The first stage, Channel Attention, aggregates tokens from different channels within the same time block to extract the signal semantics:

$$\text{ChannelAttention}(\mathcal{Q}_c, \mathcal{K}_c, \mathcal{V}_c) = \text{softmax} \left(\frac{\mathcal{Q}_c \mathcal{K}_c^T}{\sqrt{d_k}} \right) \mathcal{V}_c \quad (9)$$

where \mathcal{Q}_c , \mathcal{K}_c , and \mathcal{V}_c represent the query, key, and value matrices for the channel dimension.

In the second stage, Time Attention aggregates tokens across different time segments within the same channel to capture the full temporal semantics of the input:

$$\text{TimeAttention}(\mathcal{Q}_t, \mathcal{K}_t, \mathcal{V}_t) = \text{softmax} \left(\frac{\mathcal{Q}_t \mathcal{K}_t^T}{\sqrt{d_k}} \right) \mathcal{V}_t \quad (10)$$

where \mathcal{Q}_t , \mathcal{K}_t , and \mathcal{V}_t are the query, key, and value matrices for the time dimension.

This two-stage attention mechanism is particularly powerful as it allows the model to handle data from any combination of sensor channels efficiently, adapting to different configurations with minimal computational overhead. The reduction in complexity from $O(N^2 \times M^2)$ to $O(N^2) + O(M^2)$ is crucial in preventing computational overload, thereby enabling real-time diagnostics and prognostics across various equipment types. Moreover, by focusing attention on the most relevant parts of the input data, this mechanism significantly enhances the model's ability to extract and utilize critical features, leading to more accurate and reliable diagnosis and prognosis outcomes.

The structure of the model is illustrated in Fig. 2b. RmGPT is composed of a patch-based tokenizer and K stacked layers of the RmGPT Layer, which store the learnable prompt tokens, task tokens, and fault tokens.

3.3. Training Process

The training process of the RmGPT model involves two main stages: pretraining and prompt learning. Each stage plays a crucial role in ensuring that the model can generalize well to various diagnosis and prognosis tasks.

3.3.1. Next Signal Token Prediction Pretraining

We propose a pretraining strategy specifically designed for PHM applications, inspired by techniques from the natural language processing domain. The objective is to predict the next signal token in a sequence, which prevents the model from simply repeating patterns and forces it to learn the underlying dynamics of the system. Accurately predicting the next token indicates that the model has learned the intrinsic signal dynamics, which are crucial for representing the system health state. Formally, given a sequence of signal tokens $\{T_{s1}, T_{s2}, \dots, T_{sn}\}$, the model is trained to predict the next token T_{si+1} based on the preceding tokens $\{T_{s1}, T_{s2}, \dots, T_{si}\}$:

$$\mathcal{L}_{\text{pretrain}} = - \sum_{i=1}^n \log P(T_{si+1} | T_{s1}, T_{s2}, \dots, T_{si}; \theta_e) \quad (11)$$

where θ_e represents the pretraining parameters. This strategy effectively captures temporal dependencies and patterns within the signal data, providing a solid foundation for downstream tasks.

3.3.2. Efficient Prompt Learning

We also propose an efficient prompt learning approach to adapt the pretrained model to specific tasks with minimal additional training. This method introduces task-specific prompts into the model, guiding its adaptation process. The prompt tokens $T_p \in \mathbb{R}^{l_p \times M_i \times d}$ are added to the input sequence, effectively steering the model's attention towards task-relevant features:

$$\mathcal{L}_{\text{prompt}} = \sum_{j=1}^m \mathcal{L}_{\text{task}}(T_{sj} + T_p; \theta_p) \quad (12)$$

where θ_p represents the parameters specific to prompt learning and $\mathcal{L}_{\text{task}}$ is the loss function for the downstream task.

The advantages of this approach are twofold: (1) By fine-tuning only a few learnable embeddings, the model can efficiently adapt to various tasks and diagnosis equipment, significantly broadening its application scenarios. (2) This method enhances the model generalization performance by making minimal adjustments to the pretrained parameters obtained from vast amounts of data.

The relationship between pretraining and prompt learning is integral to the model training process. pretraining provides the model with a robust initialization, capturing general patterns in the signal data. Prompt learning allows the model to quickly adapt to new tasks with minimal data, leveraging task-specific information encoded in the prompts. This comprehensive training process ensures that the RmGPT model remains flexible and effective across a wide range of diagnosis and prognosis tasks, adapting seamlessly to different datasets and conditions.

4. EXPERIMENTS

In this section, we conduct a comprehensive evaluation of the RmGPT model across various diagnosis and prognosis tasks using diverse datasets. We begin by describing the datasets employed in our experiments, highlighting their diversity and relevance to real-world applications. Following this, we present the main results, comparing the performance of RmGPT to SOTA algorithms[20, 21, 22, 23, 24, 25, 26, 27]. Additionally, we assess the few-shot learning capabilities of RmGPT, demonstrating its effectiveness in scenarios with limited training data. Subsequently, we conduct an efficiency analysis of RmGPT during the training and inference processes. Finally, we analyze the token space representations learned by RmGPT, illustrating its ability to transform noisy input signals into a clear and distinct semantic space.

4.1. Dataset description

In this study, we employ a variety of datasets to evaluate the performance of the RmGPT model on both diagnosis and prognosis tasks. These datasets, summarized in Table 1, originate from different types of equipment and exhibit a wide range of characteristics, including signal channels, fault categories, sampling frequencies and dataset sizes.

Table 1: Overview of datasets used for diagnosis and prognosis tasks

Tasks	Object	Datasets	Classes	Channels	Total Points	Sample Frequency
Diagnosis	Bearing	CWRU[28]	16	1, 2, 3	9,011,145	12 kHz
	Bearing	SLIET[29]	13	3	13,631,475	70 kHz
	Gear	QPZZ-II[30]	5	9	1,064,960	5120 Hz
	Gear	SMU[31]	3	1	300,000	10 kHz
Prognosis	Bearing	XJTU[32]	4	2	204,046,336	25.6 kHz

The above rolling bearing and gear datasets are popular benchmark datasets that have been widely utilized to validate the effectiveness of various algorithms. However, due to the significant differences between these datasets, no previous work has attempted to use a model with the same parameters across all seven diverse datasets for both diagnosis and prognosis tasks. This study seeks to demonstrate the feasibility of constructing a unified model with consistent parameters for fault diagnosis and prognosis in rotating machinery, using these varied datasets as a preliminary validation.

4.2. Main results

In our experiments, we train the RmGPT model using a set of carefully selected hyperparameters to ensure optimal performance across various diagnosis and prognosis tasks. The experiments are conducted on a computing server equipped with 8 NVIDIA RTX 3090 GPUs.

To ensure consistency across diverse datasets, we uniformly downsampled all data to approximately 5kHz and standardized the input signal windows to 2048 time steps. This preprocessing step was essential to harmonize the datasets, allowing the model to learn underlying patterns without being influenced by variations in signal amplitude or sampling rates.

The hyperparameters employed for training the RmGPT model are outlined in Table 2. In the Tokenizer settings, both stride length and patch length were set to 256. The model architecture was designed with 4 layers and 512 hidden units, amounting to a total of 68.50M parameters, ensuring sufficient representational capacity. The prompt and fault token lengths were set to 10 and 1, respectively. During the optimization phase, the model was trained with a batch size of 256 and a learning rate of 3.00×10^{-7} . The training regimen comprised 20 epochs of pretraining, conducted as self-supervised learning across all datasets without label information, followed by 3 epochs of fine-tuning and 5 epochs of prompt learning.

We conducted a comprehensive evaluation of the RmGPT model across various diagnosis and prognosis tasks using multiple datasets. To ensure the fairness of all comparisons, the experimental setup maintained a consistent training-to-testing ratio of 8:2 across all datasets. For the RmGPT model, we conducted a single pretraining phase on all available training data, followed by supervised fine-tuning across all datasets simultaneously. This approach allows RmGPT to leverage the shared information across different datasets, enhancing its generalization capabilities. In contrast, the comparison SOTA models were individually fine-tuned on each dataset, optimizing their performance for specific tasks but lacking the unified approach inherent to RmGPT. This rigorous and consistent evaluation framework underscores the robustness and adaptability of RmGPT in diverse diagnostic and prognostic scenarios, further validating its superiority as a foundation model for rotating machinery. The results, summarized in Table 3, highlight one of the most significant contributions of our work: the ability to use a single model with the same parameters across all datasets while outperforming SOTA algorithms in diverse tasks.

In the diagnosis tasks, the RmGPT model consistently demonstrated superior performance, significantly surpassing all comparison models, particularly in challenging datasets like QPZZ and SLIET.

Table 2: Hyperparameters Used for Training RmGPT Model

Hyperparameters	
Batch Size	256
Learning Rate	3.00×10^{-7}
Pretrain Epochs	20
Finetune Epochs	3
Prompt Epochs	5
Stride Length (S)	256
Patch Length (P)	256
Layers	4
Hidden Numbers (d)	512
Prompt Token Length (l_p)	10
Fault Token Length (l_t)	1
Model Size	68.50 M

The RmGPT-Prompt configuration achieved an impressive average accuracy of 99.21% across multiple datasets, with individual dataset accuracies ranging from 98.05% to 100%. The RmGPT-Finetune configuration further improved upon this, achieving an average accuracy of 99.75% and achieving perfect scores on several datasets.

In prognosis tasks, RmGPT also excelled, particularly in predicting the Remaining Useful Life (RUL) of rolling bearings, where it outperformed all comparison models. Specifically, the RmGPT-Prompt configuration achieved a Mean Absolute Error (MAE) of 0.150 and a Mean Squared Error (MSE) of 0.033, while the RmGPT-Finetune configuration further reduced these errors to 0.136 MAE and 0.030 MSE.

The use of a single set of PHM model parameters to effectively handle diverse datasets with significant variability demonstrates the feasibility of constructing a unified PHM model for fault diagnosis and prognosis. This unified approach paves the way for creating large-scale models that can generalize across various rotating machinery.

4.3. Few-Shot Learning Capabilities

To further evaluate the adaptability and robustness of the RmGPT model, we conducted few-shot learning experiments on the CWRU dataset. In these experiments, the training samples were limited to a few examples per class. Specifically, 1-shot learning indicates that there is one sample per class for all 16 classes, resulting in a total of 16 training samples. Similarly, 4-shot learning means there are four samples per class, totaling 64 training samples, and so on. The training set was used without

Table 3: RmGPT Uses the Same Parameter Model and Outperforms SOTA Algorithms on Different Tasks and Equipments

Task	Diagnosis						Prognosis	
	Dataset	CWRU	QPZZ	SLIET	SMU	Average ACC↑	XJTU	MAE↓
Metric	Accuracy↑	Accuracy↑	Accuracy↑	Accuracy↑	Accuracy↑			MSE↓
RmGPT-Prompt	<u>99.92%</u>	100.00%	<u>98.05%</u>	<u>99.11%</u>	<u>99.21%</u>		<u>0.150</u>	<u>0.033</u>
RmGPT-Finetune	100.00%	100.00%	99.02%	100.00%	99.75%		0.136	0.030
Transformer[21]	99.39%	100.00%	91.02%	65.67%	89.02%		0.231	0.070
TICNN[25]	90.30%	90.00%	96.26%	66.67%	85.81%		0.181	0.043
CNN_LSTM[22]	86.73%	96.98%	93.85%	66.67%	86.05%		0.186	0.045
DP_MRTN[27]	100.00%	100.00%	98.33%	98.02%	99.09%		0.250	0.083
IMSFACNN[26]	98.62%	75.00%	98.11%	66.67%	84.60%		0.250	0.083
ResNet18[20]	99.71%	<u>98.03%</u>	97.66%	48.89%	86.07%		0.259	0.091
InversePINN[24]	99.48%	100.00%	96.29%	80.67%	94.11%		0.159	0.035
TARTDN[23]	91.07%	95.00%	97.94%	63.56%	86.89%		0.158	0.034

any data augmentation. The number of testing samples was kept constant at 13,734. Importantly, all methods, including RmGPT and the compared models, were evaluated without any prior exposure to additional samples from the CWRU dataset, ensuring that none of the models had seen the test data during training. Moreover, the training and testing sample sizes were kept consistent across all models to guarantee a fair comparison. This rigorous approach ensures that the observed performance differences genuinely reflect the models' capabilities in few-shot learning scenarios.

The results of the few-shot learning experiments are summarized in Table 4. RmGPT consistently outperforms other models, demonstrating its ability to achieve high accuracy with very few training samples. This superior performance can be attributed to the extensive pretraining of RmGPT on large datasets, which enables the model to learn generalizable fault signal patterns. The RmGPT model, particularly under the prompt learning configuration, shows remarkable performance even in extreme conditions. In the 1-shot scenario, RmGPT-Prompt achieves a diagnosis accuracy of 92.02% across 16 fault classes, significantly outperforming other models. In the 8-shot scenario, RmGPT-Prompt reaches an accuracy of 99.43%, further highlighting its robustness and effectiveness. These results demonstrate that RmGPT can efficiently leverage small amounts of data to achieve high-precision diagnostics. The model's exceptional performance in few-shot scenarios makes it highly suitable for practical equipment maintenance situations where fault samples are often scarce. This validates the feasibility of applying a general-purpose model like RmGPT in real-world scenarios.

Table 4: Few-shot Diagnosis Performance on CWRU Dataset

Training Data		Accuracy↑				
Setting		1-shot	4-shot	8-shot	16-shot	10% Data Full Data
RmGPT-Prompt	92.02% 97.25% 99.27% 99.43% 100.00% 99.92%					
RmGPT-Finetune	<u>65.56%</u> <u>68.84%</u> <u>72.83%</u> <u>86.86%</u> <u>99.88%</u> 100.00%					
Transformer	10.75%	15.57%	15.10%	19.75%	95.41%	99.39%
TICNN	10.76%	5.36%	10.45%	10.76%	77.00%	90.30%
CNN_LSTM	10.73%	5.54%	10.75%	10.73%	81.91%	86.73%
DP_MRTN	5.36%	21.47%	41.57%	55.36%	99.82%	100.00%
IMSFACNN	5.42%	5.42%	5.42%	5.42%	28.18%	98.62%
ResNet18	5.42%	5.29%	6.06%	5.42%	46.29%	99.71%
InversePINN	5.37%	10.78%	14.28%	5.37%	95.08%	99.48%
TARTDN	5.40%	5.40%	5.40%	5.40%	33.65%	91.07%

These results underscore the strength of RmGPT in practical scenarios, demonstrating its potential to be used as a universal model for various rotating machinery diagnostics and prognostics, even with limited fault data.

4.4. Efficiency Analysis

To evaluate the efficiency of the RmGPT model, we compared its performance under various configurations, focusing on inference time, FLOPS, backward time, and the number of training parameters. The results are summarized in Table 5.

The impact of the proposed patch-based tokenization and Time-Channel Attention mechanism on reducing computational complexity and improving performance is significant. The original configuration shows an inference time of 4.970 ms and FLOPS of 51.097 GFLOPS. Removing the patch-based tokenization increases the inference time to 337.773 ms and FLOPS to 3813.998 GFLOPS. Similarly, excluding the Time-Channel Attention mechanism results in an inference time of 9.281 ms and FLOPS of 102.214 GFLOPS. For training efficiency, the prompt learning approach is more efficient than finetuning. The backward time for prompt learning is 6.765 ms with 3.038 M training parameters, compared to 22.023 ms with 68.548 M parameters for finetuning.

Table 5: Efficiency Comparison of RmGPT

Model Efficiency			
	Orin	Without Patch	Without TC Attention
inference Time (ms)	4.970	337.773	9.281
FLOPS (GFLOPS)	51.097	3813.998	102.214
Training Efficiency			
	Prompt	Finetune	
Backward Time (ms)	6.765	22.023	
Training Parameters (M)	3.038	68.548	

The model ability to process diverse signal inputs efficiently and adapt to various tasks using prompt learning demonstrates its potential as a versatile tool for rotating machinery diagnostics and prognostics.

4.5. Token Space Analysis

To further analyze the inference process of RmGPT, we visualize the original signal samples along with the corresponding Time-Frequency Task Tokens (CLS Tokens) and Fault Tokens obtained by feeding the signals into RmGPT. We applied the t-SNE method to reduce the dimensionality of these tokens to a 2D space for visualization.

Fig. 4 shows the comparison between the original input signal space and the CLS Token space generated by RmGPT. Different categories of samples are represented by different colors. The left Figure shows the dimensionality reduction of the original signals, whereas the right Figure shows

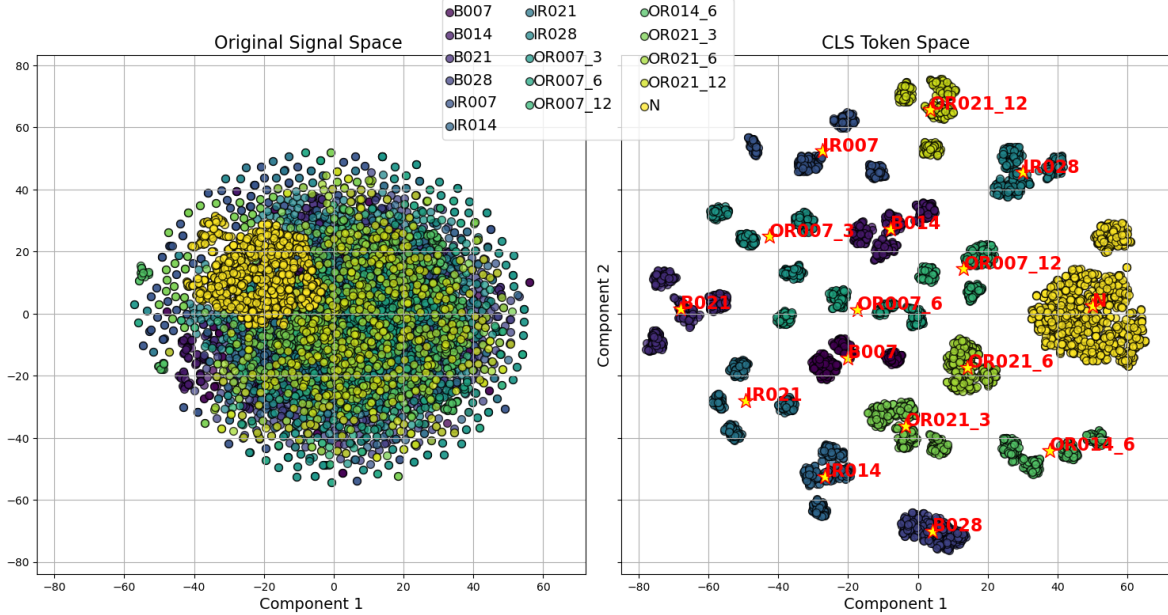


Figure 4: RmGPT can transform noisy input signals into a CLS semantic space with clear class boundaries

the dimensionality reduction of the CLS Tokens, with the positions of the Fault Tokens for different categories marked in red. The visualized CLS Token space shows the much clearer classification boundaries than the original signal space. Additionally, the model Fault Tokens learn the prototype characteristics of different categories. Different fault modes are tightly clustered around distinct class centers, indicating that RmGPT accurately learns and distinguishes the intrinsic fault patterns in the data. This clear separation of fault classes in the CLS Token space highlights the model ability to transform noisy input signals into a more structured and interpretable representation, facilitating more accurate diagnosis and prognosis.

5. Conclusion

This paper presents RmGPT, a foundation model for unified diagnosis and prognosis in rotating machinery. By utilizing a single model with consistent parameters across diverse datasets, RmGPT significantly outperforms SOTA algorithms, demonstrating exceptional accuracy and robustness in both diagnosis and prognosis tasks. The model ability to effectively handle varied equipment types, signal channels, fault categories and sampling frequencies underscores its adaptability and the feasibility of a unified approach in the PHM domain.

The result of few-shot learning experiments further highlight RmGPT capability to generalize from limited data, achieving remarkable performance even with minimal training samples. The token space analysis reveals that RmGPT transforms noisy input signals into a structured semantic space with clear class boundaries, indicating its proficiency in learning and distinguishing intrinsic fault patterns.

Future work will focus on extending RmGPT to a wider array of datasets, enhancing its generalization and scalability. Additionally, research into the local adaptation of large models will ensure their reliability

and effectiveness in diverse operational contexts. These efforts aim to establish RmGPT as a universal diagnostic tool, advancing the field of PHM and paving the way for more adaptable and generalizable diagnostic models.

6. Acknowledgements

This work was partially supported by Grant of National Natural Science Foundation (Grant No. 62371297) and Fund of Shanghai Engineering Research Center of Civil Aircraft Health Monitoring (Grant No. GCZX202204). The work of Enrico Zio is supported by iRel40 European co-funded innovation project, granted by the ECSEL Joint Undertaking (JU) under grant agreement No 876659.

References

- [1] O. Fink, Q. Wang, M. Svensén, P. Dersin, W.-J. Lee, M. Ducoffe, Potential, challenges and future directions for deep learning in prognostics and health management applications, *Engineering Applications of Artificial Intelligence* 92 (2020) 103678.
- [2] E. Zio, Prognostics and Health Management (PHM): Where are we and where do we (need to) go in theory and practice, *Reliability Engineering & System Safety* 218 (2022) 108119.
- [3] R. Liu, B. Yang, E. Zio, X. Chen, Artificial intelligence for fault diagnosis of rotating machinery: A review, *Mechanical Systems and Signal Processing* 108 (2018) 33–47. [doi:10.1016/j.ymssp.2018.02.016](https://doi.org/10.1016/j.ymssp.2018.02.016).
- [4] J. Zhang, Y. Wang, B. Jiang, H. He, S. Huang, C. Wang, Y. Zhang, X. Han, D. Guo, G. He, et al., Realistic fault detection of li-ion battery via dynamical deep learning, *Nature Communications* 14 (1) (2023) 5940.
- [5] F. Wang, Z. Zhai, Z. Zhao, Y. Di, X. Chen, Physics-informed neural network for lithium-ion battery degradation stable modeling and prognosis, *Nature Communications* 15 (1) (2024) 4332.
- [6] S. Gao, C. Feng, B. Wang, T. Yan, B. He, E. Zio, Data and Model Combined Unsupervised Fault Detection and Assessment Framework for Underwater Thruster, *IEEE Trans. Ind. Inf.* 20 (6) (2024) 8229–8238. [doi:10.1109/TII.2024.3352269](https://doi.org/10.1109/TII.2024.3352269).
- [7] Y. Wang, Z. Han, Y. Zhao, H. Wu, H.-J. Tan, Y. Zhang, Y. Li, Establishment of super sonic inlet flow pattern monitoring system: A workflow, *Aerospace Science and Technology* 120 (2022) 107297.
- [8] L. Wen, S. Su, X. Li, W. Ding, K. Feng, GRU-AE-wiener: A generative adversarial network assisted hybrid gated recurrent unit with Wiener model for bearing remaining useful life estimation, *Mechanical Systems and Signal Processing* 220 (2024) 111663. [doi:10.1016/j.ymssp.2024.111663](https://doi.org/10.1016/j.ymssp.2024.111663).

[9] Y. Wang, L. Shen, Y. Zhang, Y. Li, R. Zhang, Y. Yang, Self-supervised health representation decomposition based on contrast learning, *Reliability Engineering & System Safety* 239 (2023) 109455.

[10] J. Liang, D. Hu, Y. Wang, R. He, J. Feng, Source data-absent unsupervised domain adaptation through hypothesis transfer and labeling transfer, *IEEE Transactions on Pattern Analysis and Machine Intelligence* 44 (11) (2021) 8602–8617.

[11] J. Zhu, N. Chen, C. Shen, A new multiple source domain adaptation fault diagnosis method between different rotating machines, *IEEE Transactions on Industrial Informatics* 17 (7) (2020) 4788–4797.

[12] Y. Shi, A. Deng, X. Ding, S. Zhang, S. Xu, J. Li, Multisource domain factorization network for cross-domain fault diagnosis of rotating machinery: An unsupervised multisource domain adaptation method, *Mechanical Systems and Signal Processing* 164 (2022) 108219.

[13] Y. Xia, C. Shen, D. Wang, Y. Shen, W. Huang, Z. Zhu, Moment matching-based intraclass multisource domain adaptation network for bearing fault diagnosis, *Mechanical Systems and Signal Processing* 168 (2022) 108697.

[14] K. Sun, L. Bo, H. Ran, Z. Tang, Y. Bi, Unsupervised domain adaptation method based on domain-invariant features evaluation and knowledge distillation for bearing fault diagnosis, *IEEE Transactions on Instrumentation and Measurement* (2023).

[15] Y. F. Li, H. Wang, M. Sun, Chatgpt-like large-scale foundation models for prognostics and health management: A survey and roadmaps, *Reliability Engineering & System Safety* (2023) 109850.

[16] J. Zhou, P. Ke, X. Qiu, M. Huang, J. Zhang, Chatgpt: potential, prospects, and limitations, *Frontiers of Information Technology & Electronic Engineering* (2023) 1–6.

[17] A. Kirillov, E. Mintun, N. Ravi, H. Mao, C. Rolland, L. Gustafson, T. Xiao, S. Whitehead, A. C. Berg, W.-Y. Lo, et al., Segment anything, in: *Proceedings of the IEEE/CVF International Conference on Computer Vision*, 2023, pp. 4015–4026.

[18] Y. Wang, Y. Li, Y. Zhang, J. Lei, Y. Yu, T. Zhang, Y. Yang, H. Zhao, Incorporating prior knowledge into self-supervised representation learning for long PHM signal, *Reliability Engineering & System Safety* 241 (2024) 109602. [doi:10.1016/j.ress.2023.109602](https://doi.org/10.1016/j.ress.2023.109602).

[19] Y. Nie, N. H. Nguyen, P. Sinthong, J. Kalagnanam, A time series is worth 64 words: Long-term forecasting with transformers, in: *The International Conference on Learning Representations*, ICLR, 2022.

[20] M. Chang, D. Yao, J. Yang, Intelligent fault diagnosis of rolling bearings using efficient and lightweight resnet networks based on an attention mechanism (september 2022), *IEEE Sensors Journal* 23 (9) (2023) 9136–9145.

- [21] W. Sun, R. Yan, R. Jin, J. Xu, Y. Yang, Z. Chen, Liteformer: A lightweight and efficient transformer for rotating machine fault diagnosis, *IEEE Transactions on Reliability* (2023).
- [22] X. Chen, B. Zhang, D. Gao, Bearing fault diagnosis based on multi-scale cnn and lstm model, *Journal of Intelligent Manufacturing* 32 (2021) 971–987.
- [23] L. Cui, Z. Dong, H. Xu, D. Zhao, Triplet attention-enhanced residual tree-inspired decision network: A hierarchical fault diagnosis model for unbalanced bearing datasets, *Advanced Engineering Informatics* 59 (2024) 102322.
- [24] Y. Qin, H. Liu, Y. Wang, Y. Mao, Inverse physics-informed neural networks for digital twin-based bearing fault diagnosis under imbalanced samples, *Knowledge-Based Systems* 292 (2024) 111641.
- [25] W. Zhang, C. Li, G. Peng, Y. Chen, Z. Zhang, A deep convolutional neural network with new training methods for bearing fault diagnosis under noisy environment and different working load, *Mechanical systems and signal processing* 100 (2018) 439–453.
- [26] Z. Xu, C. Li, Y. Yang, Fault diagnosis of rolling bearings using an improved multi-scale convolutional neural network with feature attention mechanism, *ISA transactions* 110 (2021) 379–393.
- [27] Y. Chen, D. Zhang, H. Zhang, Q.-G. Wang, Dual-path mixed-domain residual threshold networks for bearing fault diagnosis, *IEEE Transactions on Industrial Electronics* 69 (12) (2022) 13462–13472.
- [28] M. Shi, C. Ding, S. Chang, C. Shen, W. Huang, Z. Zhu, Cross-domain class incremental broad network for continuous diagnosis of rotating machinery faults under variable operating conditions, *IEEE Transactions on Industrial Informatics* (2024).
- [29] A. Kumar, Y. Zhou, C. Gandhi, R. Kumar, J. Xiang, Bearing defect size assessment using wavelet transform based deep convolutional neural network (dcnn), *Alexandria Engineering Journal* 59 (2) (2020) 999–1012.
- [30] X. Li, Z. Ma, D. Kang, X. Li, Fault diagnosis for rolling bearing based on vmd-frft, *Measurement* 155 (2020) 107554.
- [31] A. H. Zamanian, Experimental dataset for gear fault diagnosis, *Dataset for Gear Fault Diagnosis* (2014) 1–2.
- [32] B. Wang, Y. Lei, N. Li, N. Li, A hybrid prognostics approach for estimating remaining useful life of rolling element bearings, *IEEE Transactions on Reliability* 69 (1) (2020) 401–412.